

## Research article

## Effects of physicochemical changes (temperature, pH, and culture media) on strong biofilm formation of *Acinetobacter baumannii* isolated from patients with respiratory infection in Iraq

Shaymaa Sabah Mutashar<sup>1</sup>, Nada H. A. L. Al-Mudallal<sup>2</sup>, Dunya Jawad Ridha<sup>3</sup>

<sup>1,3</sup>National Center for Educational Laboratories, Medical City, Ministry of Health, Baghdad, Iraq

<sup>2</sup>Department of Medical Microbiology, College of Medicine, Al-Iraqia University, Baghdad, Iraq

(Received: November 2022      Revised: January 2023      Accepted: January 2023)

Corresponding author: **Shaymaa Sabah Mutashar**. Email: sbahshyma260@gmail.com

### ABSTRACT

**Introduction and Aim:** The ability of *Acinetobacter baumannii* to form biofilms on biotic and abiotic surfaces is regulated by several pathogens' virulence factors, and this is thought to be at the root of the bacteria's resistance to antibiotics. We hope to learn how temperature, pH, and iron concentrations influence the development of biofilms in *A. baumannii* isolated from COVID-19 and non-COVID-19 individuals, and which genes are relevant for biofilm formation and antibiotic resistance.

**Materials and Methods:** Eight strong adherent isolates of *A. baumannii* from respiratory tract infection Iraqi patients (4 from COVID-19 and the other from non-COVID-19 just respiratory patients) had been used in this study which conducted from 10/1/2021 to 10/2/2022. The antibiotic sensitivity of all isolates was determined using the VITEK-2 system. The biofilm associated genes *OXA-51*, *bap*, Chaperone Usher (*CsuE*) and Integron-1, was detected using PCR. Isolates of *A. baumannii* were put through a battery of tests to determine whether they possessed the capacity to produce robust biofilms under a wide range of both physical (temperature, pH) and chemical circumstances.

**Results:** *A. baumannii* showed that all isolates were multidrug resistant and positive for the biofilm genes studied. Effect on temperature on biofilm formation showed at 44°C biofilm formation was significantly lower than that at 37°C (mean differences of 0.178000 (t= 8.355, df:3, P=0.004) and 0.204000 (t=26.521, df:3, P=0.000) respectively). The adhesion factor value in the COVID-19 positive and negative groups decreased significantly because of the pH change. Iron concentration of 60 µM significantly lowered biofilm formation among COVID-19 group and non-COVID-19 group.

**Conclusion:** *A. baumannii* are multidrug resistance isolates with a capacity to form biofilms. The ability to form biofilms by *A. baumannii* is strongly influenced by physical and chemical factors.

**Keywords:** *Acinetobacter baumannii*; antibiotic; biofilm genes; temperature; Covid-19.

### INTRODUCTION

Patients who are hospitalized to the intensive care unit are at a significant risk of contracting an infection caused by *Acinetobacter baumannii*. A significant death rate is associated with this illness, particularly in patients who are being treated in the intensive care unit (ICU). Poor outcomes are made worse by poor medication and restricted therapeutic possibilities (1). *A. baumannii* can colonize and produce biofilm on both biotic and abiotic surfaces because it encodes a wide variety of virulence genes that contribute to chronic and persistent infections, antibiotic resistance, and the ability to colonize and form biofilm on these surfaces (2). The *CsuA/BABCD* chaperone-usher pili system is responsible for the synthesis of the biofilm-associated protein (Bap), which is a surface-adhesion protein. This protein plays a key role in the start and maturation of biofilm (3). The presence of class-D OXA carbapenemase genes has been linked to the

vigorous biofilm growth caused by *A. baumannii* (4). Class I integrons are found across the MDR *A. baumannii* strain population in high numbers (5).

Alterations in the environmental conditions, both physically and chemically, have an effect not only on the phenotypic characteristics of microorganisms but also on the expression of critical functions in bacteria. The formation of biofilm is heavily influenced by a variety of environmental factors, such as temperature, osmolality, concentration of ferrous iron, availability of nutrients, quality of materials where biofilms are generated, light, and ambient acidic conditions. *A. baumannii* biofilm formation can also be affected by the surface's hydrophobicity and the amount of oxygen it contains (6).

Infections caused by *A. baumannii* have just recently been found in patients with COVID-19. These patients are given antibiotics with a broad range as a precaution, which increases the likelihood that they

will develop multidrug-resistant (MDR) bacteria. Pneumonia, which can be caused by a ventilator, can be contracted using mechanical ventilation (7). *A. baumannii* that was isolated from respiratory infected patients (both COVID-19 and non-COVID19) was studied to identify the genes that are responsible for biofilm formation and antibiotic resistance. Additionally, the effects of physicochemical changes on biofilm formation were investigated. These changes included temperature, pH, and various concentrations of iron.

## MATERIALS AND METHODS

### Bacterial isolates

Eight *A. baumannii* isolates were kindly provided by Educational Laboratories (Medical City) in Baghdad, which were isolated between January 2021 to February 2022 from respiratory sickness patients with positive Covid-19 infection or without Covid-19 infection. Each individual isolation was a potent biofilm producer. The VITEK 2 system validated the identification of *A. baumannii*. Susceptibility to antibiotics was tested using the VITEK 2 system.

### Detection of antibiotic resistance and biofilm formation genes

The *OXA-51* for bacterial genetic identification of *A. baumannii* and for antibiotic resistance, the *Bap* gene for biofilm, the Chaperone Usher (*CsuE*) for biofilm and motility, and the integron class 1 (mobile gene) for antibiotic resistance were performed on the eight isolates.

### DNA extraction and quantification

To recover DNA from each of the eight bacterial isolates, a Genomic DNA Purification Kit was utilized

(Promega, USA). To determine how much DNA was taken out of the sample, a Quantus Fluorometer was utilized. To acquire an accurate reading of the DNA concentration, 1 µl of the sample DNA was mixed with 200 µl of the diluted Quantifluor Dye. After this mixture was swirled, it was allowed to sit at room temperature for 5 minutes.

### Identification of genes *OXA-51*, *bap*, *csuE*, and integron 1

DNA extracted was used in the identification of the *OXA-51*, *bap*, *csuE* and integron1 genes by polymerase chain reaction (PCR). Table 1 contains a listing of the amplification primers for each gene, as well as the size of the product that was obtained. The polymerase chain reaction (PCR) was performed using the thermocycler (Thermo Fisher Scientific, USA) and the thermo cycling settings specified in Table 2.

### Physicochemical effects on biofilm formation

#### Temperature and pH

In this experiment, different *A. baumannii* isolates were subjected to biofilm formation tests on microtiter plate wells after being incubated at temperatures of 28, 37, and 44 °C for 24, 48, and 72 hours respectively in Luria Bertani broth. Similarly, the impact of pH on this bacterium's biofilm-forming abilities was investigated by adjusting the pH of Luria Bertani broth with 1% hydrochloric acid (HCL) or 2% sodium hydroxide (NaOH) and following the protocol for the microtiter plate assay as described by Badmasti *et al.*, (8). The PCR was applied in diagnosis of related genetic disease (9-11) and different pathogenic microorganisms (12-14)

**Table 1:** Primers sequences used in this study

Primer Name	Primer sequences (5'--3')	Annealing temp. (°C)	Product size(bp)	Ref.
OxA-51	F: TAATGCTTTGATCGGCCTTG R: TCGATTGCACTTCATCTTGG	54	353 bp	(4)
Intl -1	F: CAGTGGACATAAGCCTGTTC R: CCCGAGGCATAGACTGTA	59	160 bp	(5)
Bap	F: TGCTGACAGTGACGTAGAACCACA R: TGCAACTAGTGGAATAGCAGCCCA	60	184 bp	(8)
CsuE	F: GGCGAACATGACCTATTT R: CTCATGGCTCGTTGGTT	57	580 bp	(15)

**Table 2:** PCR Program used in molecular study

Stage	Temperature (time)
Initial denaturation	95°C (5 min)
Denaturation	95°C (30 sec)
Annealing	54, 57, 59 or 60°C (30 sec)
Extension	72°C (1 min)
Final extension	72°C (7 min)
Hold	10°C(10 min)

**Effect of ferric chloride concentrations on biofilm formation by *A. baumannii***

Microtiter plates were used by Davis *et al.*, so that they could study the formation of *A. baumannii* biofilm being affected by five different concentrations of ferric chloride: 20 μM, 40 μM, 60 μM, 80 μM and 100 μM (16). The bacteria were grown quickly on a modified M9 medium that included 0.2% glucose and 0.2% amino acids. The medium was used for a brief amount of time. After adding 20 μM, 40 μM, 60 μM, 80 μM, and 100 μM of ferric chloride, M9's adhesion was tested at each of those concentrations.

**Statistical analysis**

We utilized SPSS (version 26) and STATISTICA for data entering, verification, and analysis respectively (version 12). For the qualitative data, descriptive statistics such as frequency distribution tables, numbers, and percentages were used, but for the quantitative data, the mean, standard deviation, and range were applied. Either Student's unpaired t-test, or the Fisher Exact test was used to analyze the data and determine whether there were statistically significant differences between the groups (a substitute for the Chi-square test). Throughout the entirety of the inquiry, a P-value of 0.05 was employed as the

threshold for determining whether the results were statistically significant (17).

**RESULTS**

***A. baumannii* identification and antibiotic susceptibility testing**

The VITEK-2 system identified *A. baumannii* bacterial isolates and determined which antibiotics worked against the eight isolates. All isolates examined exhibited substantial antibiotic resistance. The isolates were resistant to piperacillin-tazobactam (PTZ), piperacillin, trimethoprim-sulfamethoxazole (TS), cefepime, cefazidime, ciprofloxacin (CIP), ticarcillin, and ticarcillin-clavulanate (TIM), however they were more sensitive to colistin (12.5% vs. 87.5%).

**Identification of biofilm associated genes in *A. baumannii***

The results of PCR technique for the eight strong biofilm formation *A. baumannii* isolates showed that all isolates have *blaOXA-51*-Like genes (carbapenem resistance genes), integron 1 gene and *Bap* gene (biofilm association protein) and seven isolates to be positive for *CsuE* gene (Table 3, Fig. 1).

**Table 3:** Distribution of genes in *A. baumannii* isolates in the study

Genes	<i>A.baumannii</i> strains positive for gene isolated from patients tested	
	Covid-19 +ve (n=4)	Covid-19 -ve (n=4)
<i>OXA51</i>	4 (100%)	4 (100%)
<i>Bap</i>	4 (100%)	4 (100%)
<i>CSUE</i>	4 (100%)	3 (75%)
<i>Integron 1</i>	4 (100%)	4 (100%)

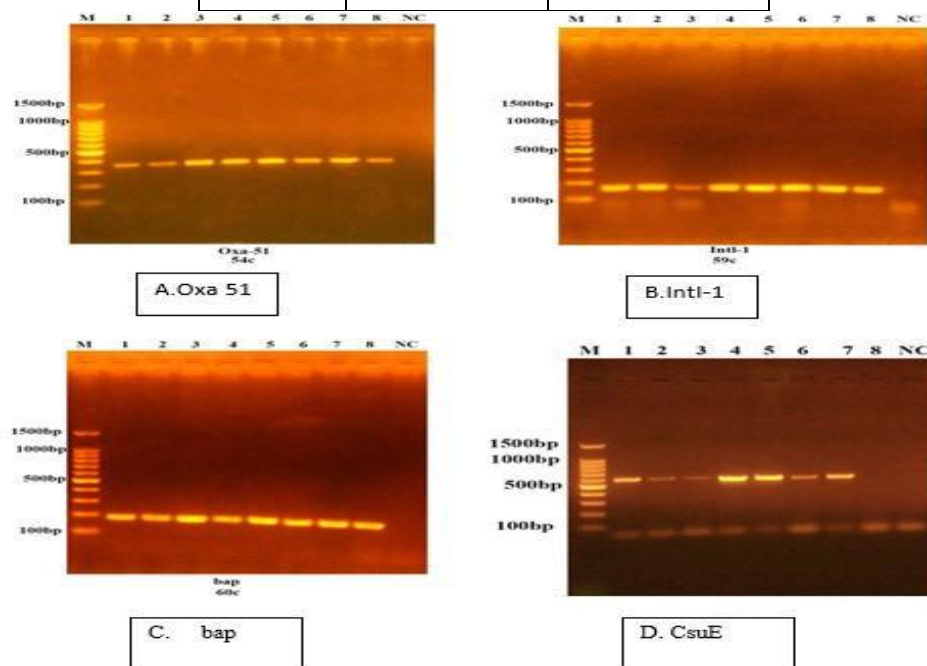


**Fig. 1:** Amplification of *Acinetobacter baumannii* genes fractionated on 1.5% agarose gel electrophoresis and stained with ethidium bromide. M: 100 bp ladder marker, NC: negative control.

**Physical and chemical effects on biofilm formation**

**Effect of temperature and pH**

In terms of physical environmental effects on biofilm formation of the eight *A. baumannii* bacterial isolates, significant differences were found in comparison to standard biofilm (37° C) among those isolated with positive Covid-19 infection or those without Covid-19. The mean values at 44° C were significantly lower than those at 37° C (0.58550 ± 0.053507 vs. 0.40750 ± 0.0142201) with significant mean differences of 0.178000 (t= 8.355, df: 3, P= 0.004). Similarly, the mean values at 44° C for non-covid-19 group was significantly lower than those at 37° C (0.52575 ± 0.041995 vs. 0.32175 ± 0.027476), with significant mean differences of 0.204000 (t= 26.521, df: 3, P=0.000). However, no significant differences were observed when the temperature was reduced to 28° C, whether in the groups with or without Covid-19 infection (P> 0.05; Table 4).

Significant differences were identified among both groups at pH 5 comparison to standard for biofilm formation by *A. baumannii* isolated from Covid-19 positive and negative groups (0.58550 ± 0.053507 vs. 0.26150 ± 0.022249) with significant mean differences of 0.324000 (t= 13.847, df: 3, P= 0.001), and (0.52575 ± 0.041995 vs. 0.25900 ± 0.032833) with significant mean differences of 0.266750 (t= 7.707, df: 3, P= 0.005) (Table 4).

Likewise, at a pH of 9 the adhesion factor value significantly decreased than that of standard for both with or without Covid-19 infection groups (0.58550 ± 0.053507 vs. 0.30875 ± 0.051299) with significant mean differences of 0.276750 (t= 11.383, df: 3, P= 0.001), and (0.52575 ± 0.041995 vs. 0.32550 ± 0.032399) with significant mean differences of 0.200250 (t= 11.369, df: 3, P= 0.001) respectively (Table 4) (Fig. 2)

**Table 4:** Comparison of adherence among *A. baumannii* isolates (n=8) following exposure to varying range of temperature and pH

Physical exposure medium	Covid-19 groups					
	Covid-19 positive (n=4)			Covid-19 negative (n=4)		
	Mean ± SD	Mean difference <sup>a</sup>	Significance <sup>b</sup>	Mean ± SD	Mean difference	Significance
37°C	0.58550 ± 0.053507	0.178000	t= 8.355, df: 3, P= 0.004	0.52575 ± 0.041995	0.204000	t= 26.521, df: 3, P= 0.000
44°C	0.40750 ± 0.0142201			0.32175 ± 0.027476		
28°C	0.56675 ± 0.062297	0.018750	t= 0.919, df: 3, P= 0.426	0.53575 ± 0.056358	-0.010000	t= -0.875, df: 3, P= 0.446
HCL	0.26150 ± 0.022249	0.324000	t= 13.847, df: 3, P= 0.001	0.25900 ± 0.032833	0.266750	t= 7.707, df: 3, P= 0.005
NaOH	0.30875 ± 0.051299	0.276750	t= 11.383, df: 3, P= 0.001	0.32550 ± 0.032399	0.200250	t= 11.369, df: 3, P= 0.001

<sup>a</sup>: Mean difference from standard value (37°C), <sup>b</sup>: One-sample t-Test.

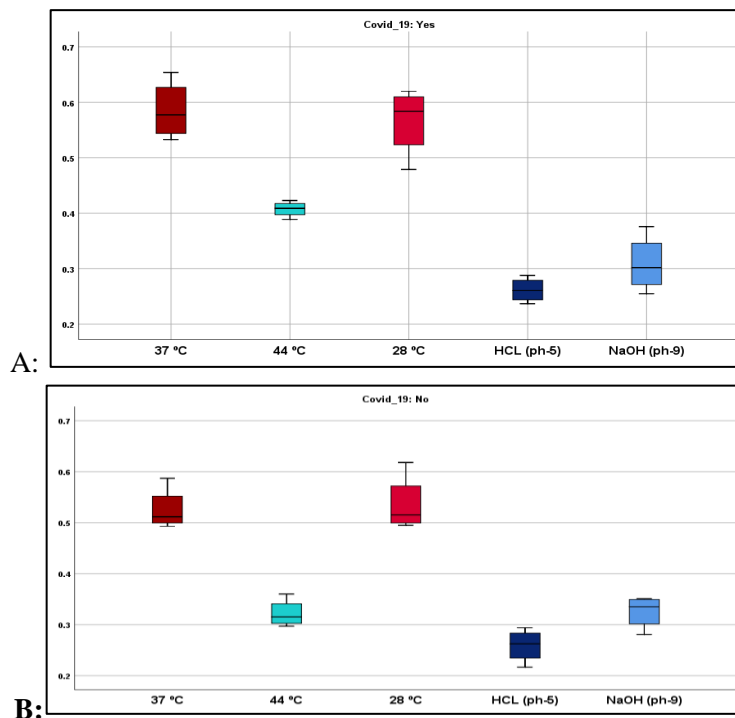


**Fig. 2:** Comparison of Means of *A. baumannii* adherence following exposure to temperature and pH changes among A: Covid-19 positive group; B: Covid-19 negative group

**Effect of varying concentration of ferric chloride on biofilm formation**

The propensity of *A. baumannii* isolates to produce biofilms on exposure to various amounts ferric chloride (FeCl<sub>3</sub>) was examined. Strains isolated from individuals infected or uninfected with COVID -19 were found to differ significantly. The mean values at concentration of 40 μM and 60 μM were significantly lower than that of standard among COVID-19 group (0.58500 ± 0.133854 vs. 0.29900 ± 0.055444) (t= 6.487, df: 3, P= 0. 007) and (0.58500 ± 0.133853 vs. 0.25000 ± 0.059939) (t= 8.655, df: 3, P= 0.003) with significant mean differences of 0.0286000 and 0.3335000 respectively. On the other hand, significant differences among non- COVID -19 group were identified at concentration of 20 μM, as its mean value

was significantly lower than that of standard (0.55975 ± 0.127573 vs. 0.40625 ± 0.072990) with significant mean differences of 0.153500 (t= 3.732, df: 3, P= 0.034). Similarly, the mean values at the concentration of 60 μM and 80 μM were significantly lower than that M9 (0.55975 ± 0.127573 vs. 0.28575 ± 0.078360) (t= 3.549, df: 3, P= 0.038) and (0.55975 ± 0.127573 vs. 0.31500 ± 0.036231) (t= 3.766, df: 3, P= 0.33) with significant mean differences of 0.274000 and 0.244750 respectively. However, the mean values at concentration of 20 μM, 80 μM, and 100 μM among COVID -19 infection group, and the mean values of 40 μM and 100 μM among non- COVID-19 infection group showed no significant differences from standard (P > 0.05) as shown in Table 5 and Fig. 3.

**Table 5:** Comparison of adherence among *A. baumannii* isolates (n=8) following exposure to varying concentration of Ferric chloride

Chemical exposure medium (FeCl <sub>3</sub> )	Covid-19 groups					
	Covid-19 positive (n=4)			Covid-19 negative (n=4)		
	Mean ± SD	Mean difference <sup>a</sup>	Significance <sup>b</sup>	Mean ± SD	Mean difference	Significance
M9	0.58500 ± 0.133853	0.140250	t= 2.878, df: 3, P= 0.064	0.55975 ± 0.127573	0.153500	t= 3.732, df: 3, P= 0.034
20 μM	0.44475 ± 0.046743			0.40625 ± 0.072990		
40 μM	0.29900 ± 0.055444	0.0286000	t= 6.487, df: 3, P= 0.007	0.31925 ± 0.036628	0.240500	t= 3.189, df: 3, P= 0.050
60 μM	0.25000 ± 0.059939	0.3335000	t= 8.655, df: 3, P= 0.003	0.28575 ± 0.078360	0.274000	t= 3.549, df:3, P= 0.038
80 μM	0.35925 ± 0.028999	0.2225750	t= 3.086, df: 3, P= 0.054	0.31500 ± 0.036231	0.244750	t= 3.766, df: 3, P= 0.33
100 μM	0.39550 ± 0.012662	0.189500	t= 2.733, df: 3, P= 0.072	0.37125 ± 0.056647	0.188500	t= 2.786, df: 3, P= 0.069

<sup>a</sup>:Mean difference from standard value (M9), <sup>b</sup>: One-sample t-Test

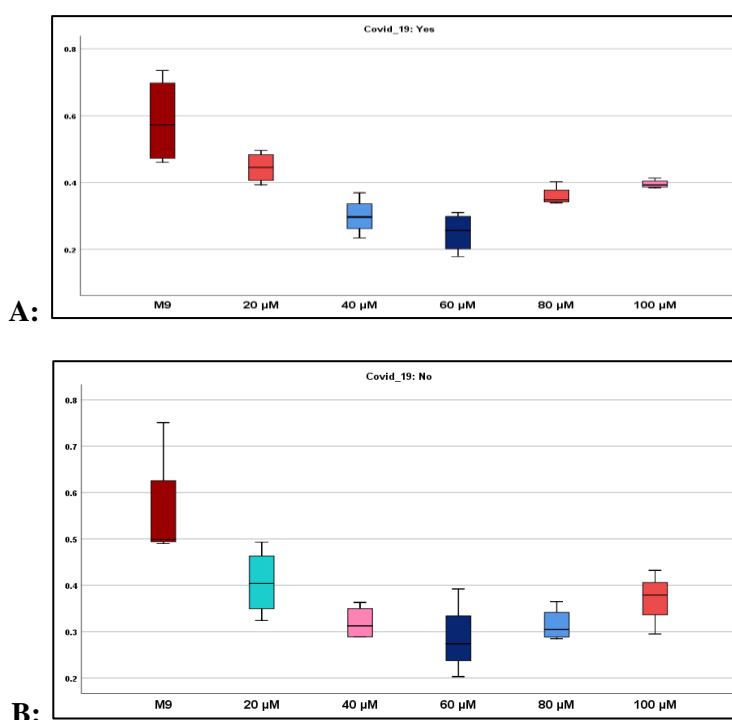


**Fig. 3:** Comparison of means of *A. baumannii* adherence following exposure to varying Ferric chloride concentrations among A: Covid-19 positive group; B: Covid-19 negative group

## DISCUSSION

The isolates in this study were confirmed as *A.baumannii* based on the detection of the carbapenem- hydrolyzing (*bla*OXA-51-Like) gene which has been used as a simple and reliable way to identify *A. baumannii* (4). The study showed the *A. baumannii* isolates (n=8) isolated from Covid-19 positive and negative individuals to be multi drug resistant (MDR). In general, the diagnosis of Covid-19 done by PCR and CT-scan techniques (18-20).

*A. baumannii* multidrug resistance and the production of biofilms have both been linked to several genes. (21). Some of the MDR and biofilm determinants identified for *A. baumannii* include the *Bap* (biofilm-associated protein), *CsuE* (Chaperone Usher protein) and mobile *Integron class 1* genes (22). All strains that were strong biofilm formers in this study were also positive for the presence of the *bap* and *csuE* and integron class 1 genes, which further confirms these strains to be biofilm formers. In *A. baumannii*, chaperone-usher pili is used in attachment and invasion, biofilm formation, cell motility and transport of proteins and DNA across membranes (23) while the integrons, which are mobile DNA elements integrate into the resistance gene cassettes, leading to resistance phenotypes (22).

The physiochemical (temperature, pH, Ferric chloride concentration) effects of biofilm formation by *A. baumannii* were also investigated in this study. Significant variations were found between isolates isolated from COVID -19 positive infections or those without, compared to the normal biofilm 37°C. No significant difference was observed with the temperature decreasing to 28° C, between the COVID -19 groups (P>0.05). *A. baumannii* biofilm development was somewhat improved when incubated at ambient temperature (28° C) as opposed to at 37°C in few of the isolates, which is agreement with a previous study (24). Our study also observed that the biofilm formation significantly decreased when the temperature was increased to 44° C. As regards to pH changes it was observed as with other bacteria *A. baumannii* also preferred a pH of 7.0 to form biofilms. An increase and decrease in pH levels led to the inhibition of biofilm formation which agrees with earlier research (25), wherein it was recorded that *A. baumannii* isolates showed maximum biofilm formation between pH 6.0-7.0 (26). This is essential because treating surfaces, such as catheters or indwelling medical devices, with alkaline solutions or cleansers may minimize the chance of bacterial colonization and subsequent infections due to biofilm.

Data obtained in this study also showed that iron chloride (ferric chloride FeCl<sub>3</sub>) inhibited biofilm formation in all five concentrations studied (Table 3). Our results agree with earlier studies, where it has

been shown that iron enhances biofilm formation with increasing concentrations altering the biofilm activity from strong to weak (27).

## CONCLUSION

It has become increasingly difficult for antimicrobial drugs to combat isolates that form biofilms, prompting the creation of novel therapeutic strategies. Temperature, acidity, alkalinity, and high iron concentrations are physical and chemical factors that affect biofilm formation. These factors play a significant regulatory role in antibiofilm activity, which helps to prevent infection associated with medical equipment that is brought on by biofilms.

## CONFLICT OF INTEREST

Authors declare no conflicts of interest.

## REFERENCES

1. Tacconelli, E., Göpel, S., Gladstone, B.P., Eisenbeis, S., Hölzl, F., Buhl, M., et al., Development and validation of BLOOMY prediction scores for 14-day and 6-month mortality in hospitalised adults with bloodstream infections: a multicenter, prospective, cohort study. *The Lancet Infectious Diseases*. 2022; 22(5): 731-741.
2. Thummeepak, R., Kongthai, P., Leungtongkam, U., Sitthisak, S. Distribution of virulence genes involved in biofilm formation in multi-drug resistant *Acinetobacter baumannii* clinical isolates. *Int Microbiol*. 2016; 19(2): 121-129.
3. Elkheloui, R., Laktib, A., Mimouni, R., Aitalla, A., Hassi, M., Elboulani, A., et al., *Acinetobacter baumannii* biofilm: Intervening factors, persistence, drug resistance, and strategies of treatment. *Mediterranean Journal of Infection, Microbes and Antimicrobials*. 2020; 9(7):1-12.
4. Morovat, T., Bahram, F., Mohammad, E., Setareh, S., Mehdi, F.M. Distribution of different carbapenem resistant clones of *Acinetobacter baumannii* in Tehran hospitals. *The New Microbiologica*. 2009; 32(3): 265-271.
5. Azizi, M., Mortazavi, S.H., Etemadimajed, M., Gheini, S., Vaziri, S., Alvandi, A., et al., Prevalence of extended-spectrum β-Lactamases and antibiotic resistance patterns in *Acinetobacter baumannii* isolated from clinical samples in Kermanshah, Iran. *Jundishapur Journal of Microbiology*, 2017; 10(12): e61522.
6. Toyofuku, M., Inaba, T., Kiyokawa, T., Obana, N., Yawata, Y., Nomura, N. Environmental factors that shape biofilm formation. *Bioscience, Biotechnology, and Biochemistry*. 2016; 80(1): 7-12.
7. Lima, W.G., Brito, J.C. M., da Cruz Nizer, W. S. Ventilator-associated pneumonia (VAP) caused by carbapenem-resistant *Acinetobacter baumannii* in patients with COVID-19: Two problems, one solution? *Medical hypotheses*. 2020;144: 110139.
8. Badmasti, F., Siadat, S.D., Bouzari, S., Ajdary, S., Shahcheraghi, F. Molecular detection of genes related to biofilm formation in multidrug-resistant *Acinetobacter baumannii* isolated from clinical settings. *Journal of Medical Microbiology*. 2015; 64(5): 559-564.
9. Hamoode, R.H., Alkubaisy, S.A., Sattar, D.A., Hamzah, S.S., Saleh, T.H., Al-Rubaii, B.A.L. Detection of anti-testicular antibodies among infertile males using indirect immunofluorescent technique. *Biomedicine (India)*.2022; 42 (5):978-982.
10. Ali, S.M., Lafta, B.A., Al-Shammary, A.M., Salih, H.S. In vivo oncolytic activity of non-virulent Newcastle disease virus Iraqi strain against mouse mammary adenocarcinoma. *AIP Conference Proceedings*. 2021; 2372: 030010.

11. Ali, S.M., Laftah, B.A., Al-Shammary, A.M., Salih, H.S. Study the role of bacterial neuraminidase against adenocarcinoma cells *in vivo*. In AIP Conference Proceedings 2021; 2372; 030009.
12. Al-Rubaii, B.A.L. Cloning LasB gene of *Pseudomonas aeruginosa* elastase 10104-2aI in *E. coli* BL21 and *E. coli* DH5a and investigated their effect on the stripping of Vero cells. *Pakistan J Biotechnol.* 2017; 14(4):697-705.
13. Shehab, Z.H., Laftah, B.A. Correlation of nanI (Neuraminidase) and production of some type III secretion system in clinical isolates of *Pseudomonas aeruginosa*. *Biomed res.* 2018; 15(3):1729-1738.
14. Saleh, T., Hashim, S., Malik, S.N., Al-Rubaii, B.A.L. The impact of some nutrients on swarming phenomenon and detection of the responsible gene *RsbA* in clinical isolates of *Proteus mirabilis*. *Int J Pharm Sci Res.* 2020;1(6):437-444.
15. Turton, J. F., Gabriel, S. N., Valderrey, C., Kaufmann, M.E., Pitt, T.L. Use of sequence-based typing and multiplex PCR to identify clonal lineages of outbreak strains of *Acinetobacter baumannii*. *Clinical Microbiology and Infection.* 2007;13(8): 807-815.
16. Davis, L., Dibner, M., Battey, J. F. Basic Methods in Molecular Biology Elsevier, New York, 1986.
17. Elliott, A.C., Woodward, W.A. Quick Guide to IBM® SPSS®: Statistical analysis with step-by-step examples. SAGE Publications, 2019.
18. Rasoul, L.M., Nsaif, M.M., Al-Tameemi, M.T., Al-Rubaii, B.A.L. Estimation of primer efficiency in multiplex PCR for detecting SARS-Cov-2 variants. *Bionatura.*2022; 7(3):1- 4.
19. Ahmed, A.W., Ahmed, R.N., Naif, M.M., Alchalabi, G.B., Mohammed, A.G. Chest CT findings and experience in 100 COVID19 patients in Mosul city, Iraq. *Biomedicine (India)*, 2021; 41(4):793-798.
20. Suhail, H.A., Abdulrahman, D.M., Ahmed, A.W. Fetal Biometry and Doppler Assessment of Pregnant Women with COVID-19. *International Journal of Biomedicine.* 2022; 12(4):554-559
21. Álvarez-Fraga, L., Rumbo-Feal, S., Pérez, A., Gomez, M.J., Gayoso, C., Vallejo, J.A., *et al.*, Global assessment of small RNAs reveals a non-coding transcript involved in biofilm formation and attachment in *Acinetobacter baumannii* ATCC 17978. *PLoS One.* 2017;12(8): e0182084.
22. Mahmood, S.S. The prevalence of integron classes genes among *A. Baumannii* isolates. *Iraqi Journal of Science.* 2022; 63(5). 1955-1960.
23. Monfared, A.M., Rezaei, A., Poursina, F., Faghri, J. Detection of genes involved in biofilm formation in MDR and XDR *Acinetobacter baumannii* isolated from human clinical specimens in Isfahan, Iran. *Archives of Clinical Infectious Diseases*, 2019;14(2): e85766.
24. Eze, E.C., El Zowalaty, M.E. Combined effects of low incubation temperature, minimal growth medium, and low hydrodynamics optimize *Acinetobacter baumannii* biofilm formation. *Infection and Drug Resistance.* 2019; 12: 3523-3536.
25. Pour, N.K., Dusane, D.H., Dhakephalkar, P.K., Zamin, F.R., Zinjarde, S.S., Chopade, B.A. Biofilm formation by *Acinetobacter baumannii* strains isolated from urinary tract infection and urinary catheters. *FEMS Immunology & Medical Microbiology.* 2011; 62(3): 328-338.
26. Nostro, A., Cellini, L., Di Giulio, M., D'Arrigo, M., Marino, A., Blanco, A.R., *et al.*, Effect of alkaline pH on staphylococcal biofilm formation. *APMIS*, 2012; 120(9): 733-742.
27. Modarresi, F., Azizi, O., Shakibaie, M.R., Motamedifar, M., Mosadegh, E., Mansouri, S. Iron limitation enhances acyl homoserine lactone (AHL) production and biofilm formation in clinical isolates of *Acinetobacter baumannii*. *Virulence.* 2015; 6(2): 152-161.